Ocean Dynamics (2001) 52: 2–10

Arnold L. Gordon · R. Dwi Susanto

Banda Sea surface-layer divergence

Received: 21 May 2001 / Accepted: 2 August 2001

Abstract Sea-surface temperature (SST) within the Banda Sea varies from a low of 26.5 °C in August to a high of 29.5 °C in December and May. Ekman upwelling reaches a maximum in May and June of approximately 2.5 Sv ($Sv = 10^6$ m^3 s^{-1}) with Ekman downwelling at a maximum in February of approximately 1.0 Sv. The Ekman pumping annual average is 0.75 Sv upwelling. During the upwelling period, from April through December the average Ekman upwelling velocity is 2.36×10^{-6} m s^{-1} (1.27 Sv). ENSO modulation is generally within 0.5 Sv of the mean Ekman curve, with weaker (stronger) July to October upwelling during El Niño (La Niña). Combined TOPEX/POSEIDON and ERS 1993–1999 altimeter data reveal a 33 cm maximum range of sea level. Steric effects are minor, with well over 80% of the sea level change due to mass divergence (some bias due to unresolved tidal aliasing may still be present). The annual and interannual sea level behavior follows the monsoonal and ENSO phenomena, respectively. Lower (higher) sea level occurs in the southeast (northwest) monsoon and during El Niño (La Niña) events. The surface-layer volume anomaly and the surface-layer divergence, assuming a two-layer ocean, are estimated. Maximum divergence is attained during the transitional monsoon months of October/November: 1.7 Sv gain (convergence), with matching loss (divergence) in the April/May. During the El Niño growth period of 1997 the surface layer is divergent, but in 1998 when the El Niño was on the wane, the average rate of change is convergent. Surface-layer divergence attains values as high as 4 Sv. Banda Sea surface-water divergence correlates reasonably well with the 3-month lagged export of surface (upper 100 m) water into the Indian Ocean as estimated by a shallow pressure gauge array. It is concluded that the Banda Sea surface-layer divergence influences the timing and transport profile of the Indonesian throughflow export into the Indian Ocean, as proposed by Wyrtki in 1958, and that satellite altimetry may serve as an effective means of monitoring this phenomena.

Keywords Indonesian seas · ENSO · Monsoon · Upwelling · Sea level

Responsible Editor: Rosemary Morrow

A. L. Gordon (✉) · R. D. Susanto
Lamont-Doherty Earth Observatory of Columbia University, Palisades, NY, USA 10964-8000
e-mail: agordon@ldeo.columbia.edu

1 Introduction

The Banda and Arafura Seas, within the rectangular region from 3.5°S to 7.5°S and 123.5°E to 134.5°E (Fig. 1a), encompass an area of 0.54 million km^2. The Banda Sea is subjected to winds from the west from November to March (northwest monsoon), and from the east from May to September (southeast monsoon). October and April are transitional months. Peak winds are attained in February and again in July. Except for the 1.7 Sv ($Sv = 10^6$ m^3 s^{-1}) export through the Lombok Strait, the Indonesian Throughflow (ITF) of 10–15 Sv transits the Banda Sea before export to the Indian Ocean (Gordon and Fine 1996; Gordon et al. 1999; Gordon 2001). As the Banda/Arafura Seas stratification and circulation exhibit strong seasonality in response to the monsoon climate forcing, Wyrtki (1958) speculates that these seas influence the character of the ITF. He proposes that during the northwest monsoon, surface water flowing into the Banda Sea from the Flores Sea sinks to greater depths, with only part of that water exported from the Banda Sea within the surface layer via the Halmahera and Maluku Seas to the north, or via the Timor Current to the south. During the southeast monsoon, "...the Timor Current flowing into the Indian Ocean takes water out of the Arafura Sea (eastern Banda Sea)...compensated by upwelling in the Banda and Arafura Seas." We investigate the Wyrtki concept using satellite-derived altimetric data.

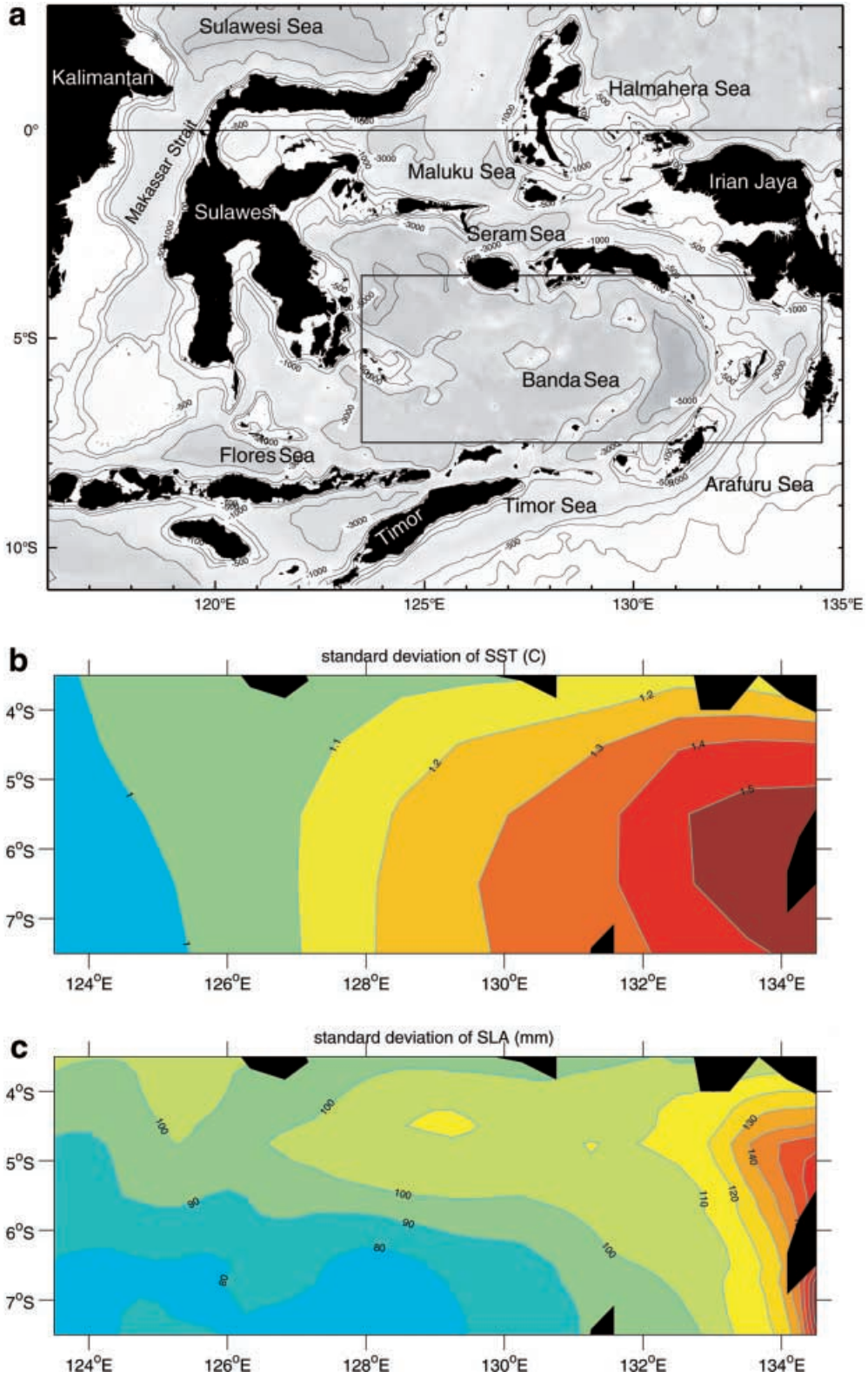

Fig. 1 **a** Eastern Indonesian seas. The isobaths are in meters. The *boxed area* 3.5°S to 7.5°S, from 123.5°E to 134.5°E, encompassing the Banda Sea and Arafura Sea, represents the study area. **b** Standard deviation of sea surface temperature within the Banda and Arafura Seas within the period 1982 to 2000. The contour interval is 0.1 °C. **c** Standard deviation of sea-level anomaly derived from the combined TOPEX/POSEIDON and ERS satellites, within the Banda and Arafura Seas within the period 1992 to 2000. The contour interval is 10 mm

The altimetric data is derived from combined TOPEX POSEIDON (T/P) and European Research Satellite (ERS) sea-level anomaly (SLA) products that have been produced by the CLS Space Oceanography Division as part of the European Union Environment and Climate project AGORA and DUACS. The SLA is obtained using an improved space/time objective analysis method which takes into account long wavelength errors (i.e., correlated noise). The correlation length for the tropical region (between 14°N and 14°S) is 350 km

(zonal direction) and 250 km (meridional direction). The method is described in Le Traon et al. (1998). The altimetric data is presented at 0.25° longitude by 0.25° latitude resolution. The T/P-ERS have been corrected for ocean tide, as the annual cycle is influenced by errors in K1 and P1 from ERS measurements, the semiannual cycle is influenced by K1 (T/P) and K2 (ERS) (see Le Provost 2001). However, as of yet, there is no high-resolution tidal model of the Indonesian seas that would allow for an estimate of remaining tidal signatures; thus, some bias due to tidal aliasing may still be present.

The sea-surface temperature (SST) and wind data are presented to define the nature of the seasonal variability in order to place the altimeter results into the proper climate context. The SST data from 1982 to 2000 are derived from the weekly optimal interpolation SST analysis (Reynolds and Smith 1994) on a 1° latitude/longitude grid. The wind data from 1949 to 2000, gridded at a scale of roughly 1.9° of latitude and longitude, is a product of the NCEP/NCAR Reanalysis Project, a joint effort between the National Center for Environmental Prediction (NCEP) and the National Center for Atmospheric Research (NCAR; Kalnay et al. 1996). In this study we use the wind data from 1982 to 2000 to synchronize with the period of the SST record.

2 Sea surface temperature and Ekman upwelling

The greatest variability of SST in the Banda Sea occurs in the eastern Banda and Arafura Sea (Fig. 1b). The SST averaged over the Banda Sea region (boxed area shown in Fig. 1a) from 1982 to 2000 displays an annual cycle from a high of 29.0 to near 30 °C from late November to mid-May, to a low of 26.5 °C in August (Fig. 2a; Ffield and Gordon 1996). The standard deviation of SST spans the SST curve for the altimeter period of 1993 to 1999, indicating that the SST during the altimeter record is not anomalous. There are two peaks in sea-surface temperature, one in early December and the other around 1 May, with a 0.5 °C SST saddle in late February to early March. The February/March cooling is most likely a product of stronger winds during February, marking the mature northwest monsoon phase. As the region is subjected to ENSO phenomena, we plot SST during El Niño and La Niña periods (Fig. 2a). El Niño is defined when the nino3 index (nino3, a standard indicator of the ENSO phase, is the SST anomaly averaged over the eastern Pacific ocean from 150°W to 90°W and 5°S to 5°N) is greater than +1.0 standard deviation; La Niña is defined as nino3 of less than −0.5 standard deviation. The number of El Niño and La Niña events from 1982 to 2000 determined by this method corresponds to the recognized occurrences, the El Niño: 1982/83, 1986/87, 1992/93, and 1997/98 and La Niña: 1985/86, 1988/89, 1996/97, and 1999/2000. During El Niño the August minimum is about 0.7 °C cooler and delayed by approximately 2 weeks from the 1982–2000 average. During La Niña the August condition is slightly warmer than average, with the minimum occurring about 2 weeks prior to the average minimum. In February and May, the El Niño SST is slightly warmer than the average SST, with La Niña having cooler SST in March and April.

The SST variability is related to thermocline depth changes, which vary with the monsoon and with ENSO (Bray et al. 1996; Ffield et al. 2000). Bray et al. (1996), using all available XBT data, find that the 21 °C isotherm depth in the Banda Sea averages between 110 to 120 m, which is shallower by 10 to 20 m than its depth in the adjacent Pacific and Indian Oceans (their Fig. 3). Thus, the Banda Sea thermocline is elevated, which is consistent with the regional cyclonic gyre as deduced from water mass analysis (Gordon and Fine 1996). Ffield et al. (2000), using XBT data in the Flores Sea, west of the Banda Sea, find a correlation of thermocline depth and ENSO (0.77 correlation of the temperature at 100 m to the Southern Oscillation Index). The 1-year running mean temperature at 100 m varies between 19 and 25 °C from 1985 to 1999 (their Fig. 5), which, on using the regional mean temperature profile data, corresponds to a depth oscillation of 60 m associated with ENSO.

Inspection of the average CTD profiles (both the up and down traces were used) of 77 Banda Sea CTD stations obtained by the Arlindo program (Gordon and Fine 1996) in August 1993 with profiles from a like number of stations at the same positions in February 1994 were used to estimate the seasonal thermocline displacement by Ilahude and Gordon (1996). They find that the seasonally averaged CTD thermocline varies in depth by 40 m between northwest and southeast monsoon, and is shallower during the cool SST phase of the southeast monsoon. A 40-m vertical displacement during a 6-month period yields an average vertical velocity of 2.5×10^{-6} m s^{-1}. However, higher-frequency oscillations of the thermocline due to internal waves and tides produce much larger displacements (Ffield and Gordon 1996). The 18 °C isotherm (midthermocline) depth variability based on the Arlindo CTD stations in the Banda Sea is 103 m, with a mean depth of 143 m.

Ekman pumping is strongest over the eastern Banda and Arafura Sea (Fig. 1c), as suggested by Wyrtki (1958). The wind stress curl induces Ekman upwelling from April through December, with weaker downwelling for the rest of the year (Fig. 2b). Maximum upwelling occurs in May and June, with a weak secondary peak in October to November. Maximum downwelling occurs in February. The annual average Ekman pumping is upwelling of 0.75 Sv. During the upwelling period from April through December the average upwelling is 1.27 Sv, amounting to an average vertical velocity of 2.36×10^{-6} m s^{-1}, close to the thermocline displacement rate of 2.5×10^{-6} m s^{-1} determined from hydrographic stations. During the altimeter period, 1993–1999, upwelling is slightly higher than the longer-term mean, where annual mean upwelling is 0.94 Sv, with an April through December upwelling of 1.44 Sv (vertical

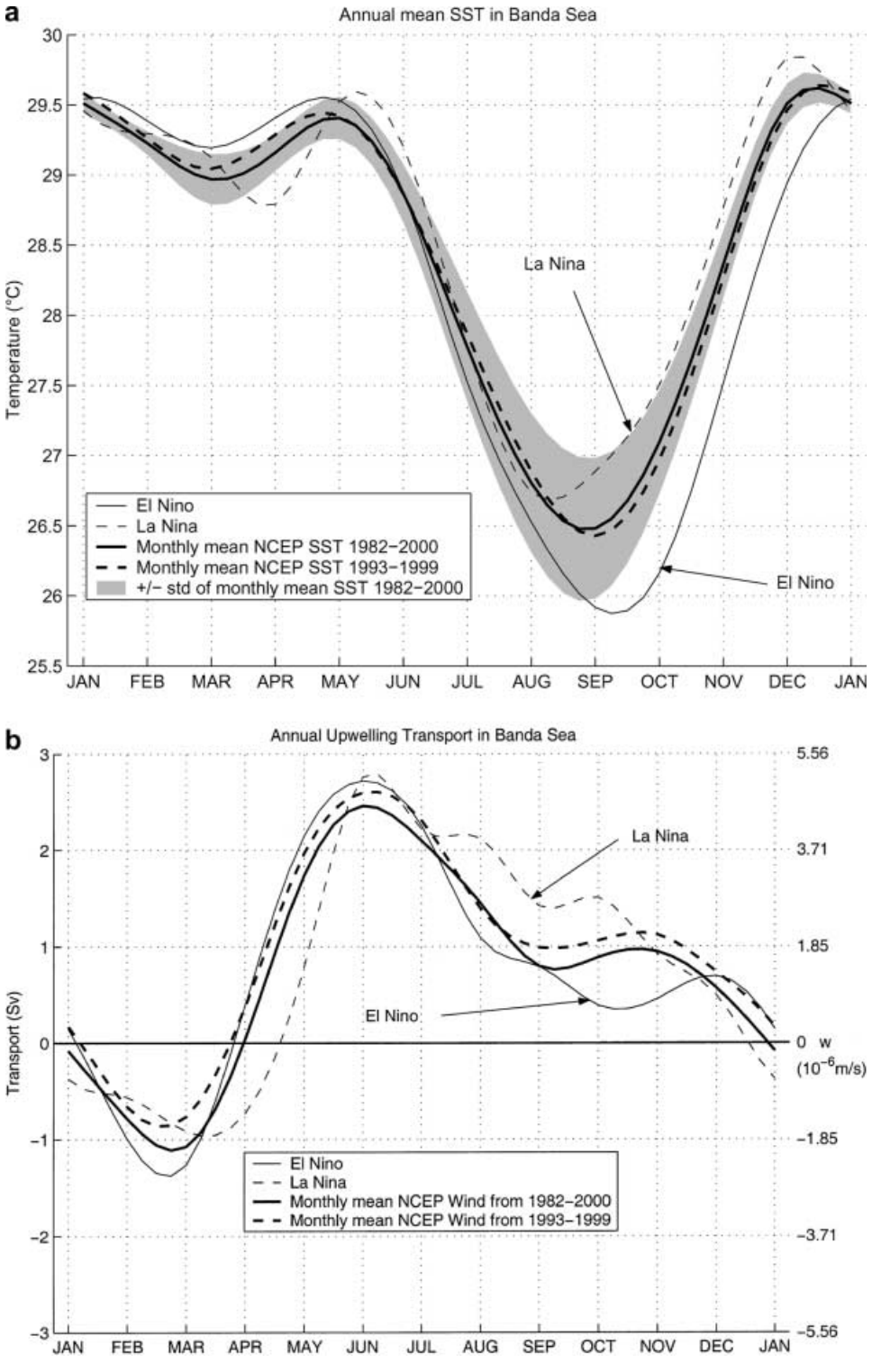

Fig. 2 **a** Annual mean sea-surface temperature (SST) within the study area (Fig. 1a). The SST data is derived from the 1982 to 2000 weekly optimal interpolation analysis of Reynolds and Smith (1994) on a 1° grid. The *gray tone* denotes the 1 standard deviation envelope. El Niño is defined when the nino3 SST anomaly is greater than +1.0 standard deviation; La Niña is defined when nino3 SST anomaly is less than −0.5 standard deviation. The SST curve is also shown for the altimeter period, from January 1993 to December 1999. **b** Ekman pumping within the study area (Fig. 1a) during 1982 to 2000. The wind data is derived from the NCEP/NCAR Reanalysis Project, Kalnay et al. (1996). El Niño is defined when nino3 SST anomaly is greater than +1.0 standard deviation; La Niña is defined when nino3 SST anomaly is less than −0.5 standard deviation. The Ekman pumping curve is also shown for the altimeter period, from January 1993 to December 1999

velocity of 2.67×10^{-6} m s^{-1}). Ekman pumping is modified during the ENSO phases, though generally remains within 0.5 Sv of the mean curve. From July to November, upwelling is reduced during El Niño and enhanced during La Niña (Fig. 2b). During La Niña the start of the upwelling season is delayed by 1 month.

In the mean, Ekman upwelling corresponds to cooler SST and shallower thermocline, as the Banda Sea responds to local forcing. However, at ENSO scales, this relationship does not hold: coolest SST of the southeast monsoon occurs at times of El Niño weaker upwelling, with warmer than normal southeast monsoon SST

occurring during the stronger upwelling of La Niña. The ENSO-related interannual variability of Banda Sea SST is most likely due to variability of thermocline depth responding to remote forcing of the larger-scale ENSO dynamics.

The cool upwelled water must be warmed to the surface-layer temperature. A rough estimate of the depth from which the Ekman upwelling is drawn may be made as follows. The mean annual surface-layer temperature is 28 °C (Fig. 2a). Estimates of the annual mean atmosphere to ocean heat flux is about 40 W m^{-2} (Fig. 1.6 of Tomczak and Godfrey 1994). Using the annual Ekman upwelling rate of 0.75 Sv (for the period 1982–2000) or 0.94 Sv (1993–1999 altimeter data period) and accepting the 40 W m^{-2} air–sea heat flux, we infer that the ocean layer supplying the water upwelling into the surface layer is derived from the 20 to 23 °C layer, from the upper thermocline.

3 Surface-layer volume and divergence

We examine the SLA over a 7-year interval from January 1993 to December 1999 inclusive, within the Banda/Arafura Seas (boxed area shown in Fig. 1a). The SLA is the deviation from the T/P-ERS 3-year mean, from December 1992 to December 1995. The SLA is converted to surface-layer volume using a simple two-layer model. The surface-layer divergence and the possible role of the Banda Sea in modifying the phasing of the surface component of the ITF are investigated. The SLA time series averaged over the Banda Sea for the period January 1993 to December 1999 (Fig. 3) reveals an annual cycle plus significant interannual variability. The maximum range (trough to peak) of the 7-year SLA time series is 33 cm. The annual range is about 20 cm with lowest sea level in the cold SST period, when the thermocline is shallowed, as expected from hydrostatic adjustment. The interannual trend, not surprisingly, is associated with ENSO (represented by the nino3 index, Fig. 3), with higher sea level during La Niña and lower in El Niño, as also noted by Bray et al. (1996). Sea level fell by 30 cm from early 1997 to late summer 1997, as the strongest El Niño in recent times evolved.

The SLA represent a combination of mass divergence, steric changes, and remaining tidal signals. How much can be attributed to steric change? Separating the steric from the isopycnal displacement contributions to SLA becomes a very entangled process. As the steric component is forced by sea–air heat flux, Q_f, we use the seasonal SST variability of 3 °C to provide a reasonable approximation of its contribution. Assuming little seasonality in salinity and that the 3 °C change extends to the full mixed layer of approximately 40 m, we find an annual steric SLA range of 2.7 cm, only 8.5% of the observed annual range of SLA. This is equivalent to a Q_f annual range (difference between lowest and highest Q_f) of 31 W m^{-2}, which is superimposed on the annual average Q_f of 40 W m^{-2}. Below 40 m the variations in temperature–salinity relationship are much reduced (Ilahude and Gordon 1996), meaning that stratification changes are due mostly to isopycnal displacement. However, if we allow for an additional seasonal change in temperature from the 40 to 150-m depth interval, diminishing from 3 °C at 40 m to 0 °C at 150 m (which

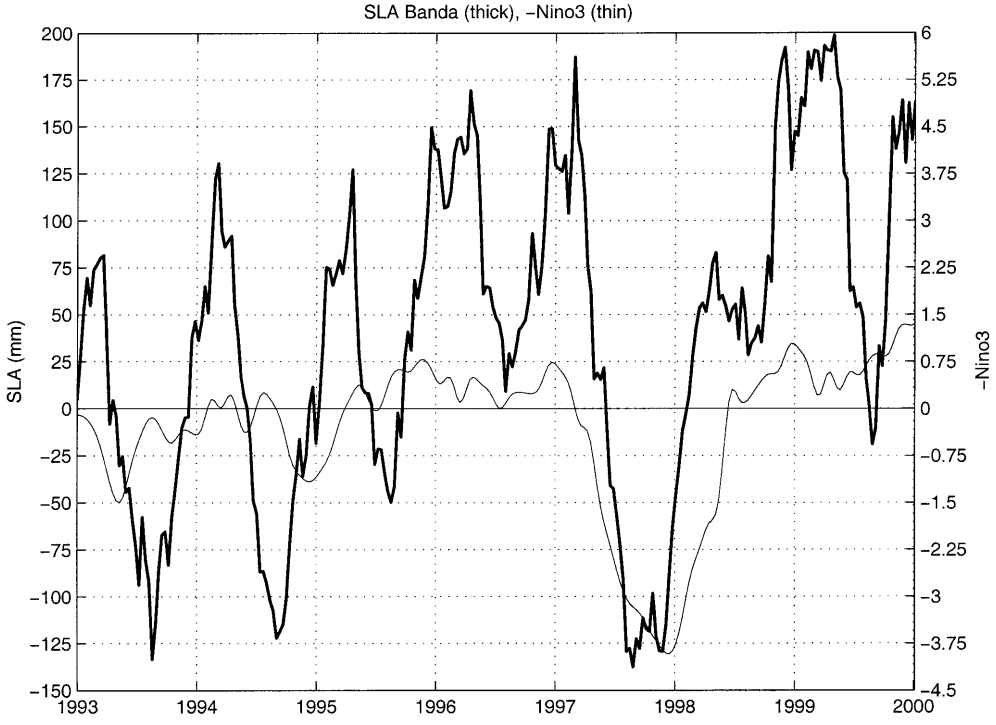

Fig. 3 Time series of sea-level anomaly (SLA) averaged within the box shown in Fig. 1. The values represent the deviation from the 3-year (December 1993 to December 1995) mean of the combined TOPEX POSEIDON/ERS altimeter data. The SLA data is generated by CLS-CNES, France. Nino3 SST anomaly is shown as the *finer line*

converts to a Q_f annual range of 65 W m^{-2}), the steric change amounts to 17% of the SLA maximum range. It is concluded that most (well over 80%) of the SLA variability can be attributed to mass divergence and any remaining tidal aliasing.

To convert sea-level changes to a volume of the surface layer, a simple two-layer stratification model is applied, a buoyant surface layer over a denser deep layer, with the pycnocline forming the discontinuity between the layers (Fig. 4). The depth of the discontinuity is taken as 150 m, the approximate mid-depth of the pycnocline. The two layers are structured to preserve the mean water column mass. The density of the upper layer is 1022.30 kg m^{-3} and for the lower layer density is 1026.85 kg m^{-3}. From the hydrostatic equation, the depth changes or heaving of the discontinuity are linearly related to change in sea level, derived from the hydrostatic relationship:

$$\Delta h = \Delta P z \, (\Delta \rho / \rho) \ ,$$

where Δh is the change in sea level associated with a change in pycnocline depth, ΔPz. The observed 33 cm maximum range of SLA over the 7-year period requires a pycnocline depth change of 75 m. This is somewhat less than the pycnocline heaving of 103 m mentioned above, but higher-frequency oscillations as internal waves would not be reflected in the Banda Sea average portrayed by the satellite altimetric-derived SLA. The Arlindo CTD data indicate some deviation (flexing) of the pycnocline shape, signifying higher-order baroclinic modes. A three-layer hydrostatic model would be needed to include these features in a sea level expression. An estimate of typical higher-order term results would alter the simple two-layer solution to a minor extent, $< 10\%$.

Using the two-layer model, the T/P-ERS-derived SLA is converted into a 7-year time series of the surface-layer volume anomaly from the 3-year mean (Fig. 5a). As expected from the thermocline depth variations, the maximum surface-layer volume occurs in February to March, with a minimum in August to September. The maximum range of the volume anomaly is 3.7×10^{13} m^3. The annual cycle (Fig. 5b) is approximated using least-squares fit of a 12-month sinusoidal wave of an amplitude to minimize the residual. The maximum and minimum volume anomalies occur in February and August, respectively. The average of the annual cycle need not be zero, as the 7-year SLA time series is the difference from a 3-year mean. The average annual cycle is positive (Fig. 5b), because of the longer duration of La Niña and higher sea-level conditions (1996 into 1997, and late 1998 to 2000). Removing the annual curve from the total volume anomaly leaves the residual (Fig. 5c) representing the nonannual variability. We find that the residual is closely coupled to the ENSO (nino3) phase, with a correlation coefficient of 0.75.

The time rate of change of the surface volume anomaly (Fig. 5a) represents a combination of mass divergence, steric changes within the surface layer, and remaining tidal aliasing. It is estimated that the steric

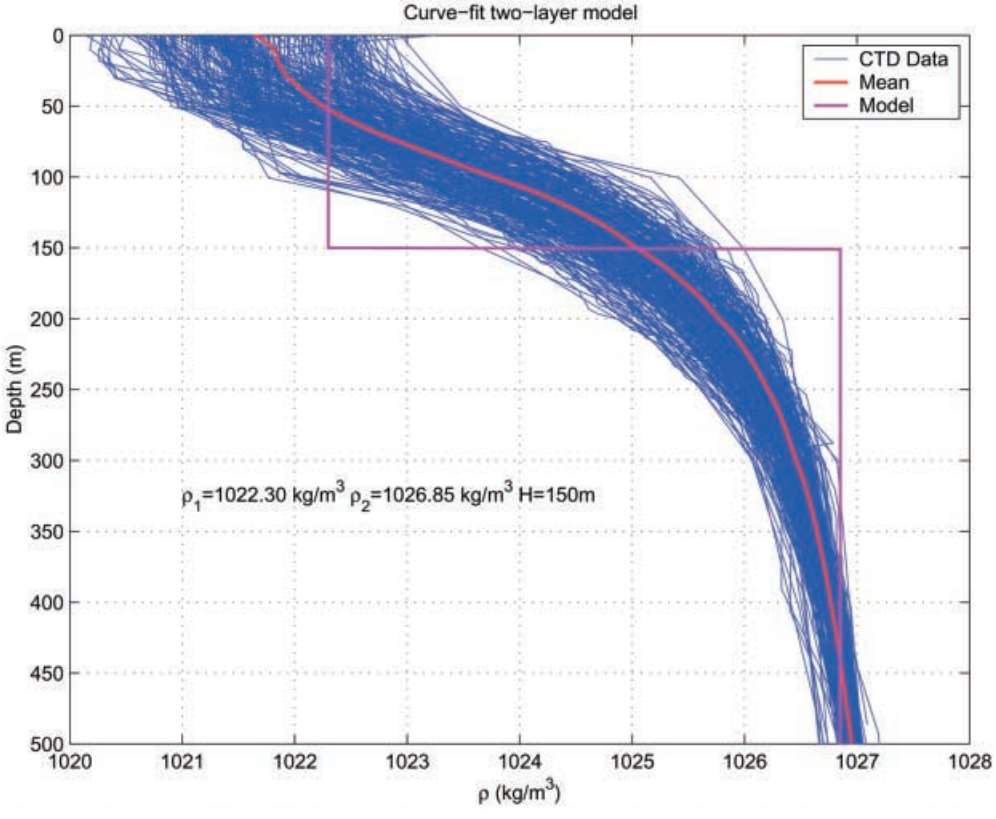

Fig. 4 Density stratification and two-layer model representation used to convert SLA to volume anomaly of the surface layer in the Banda Sea

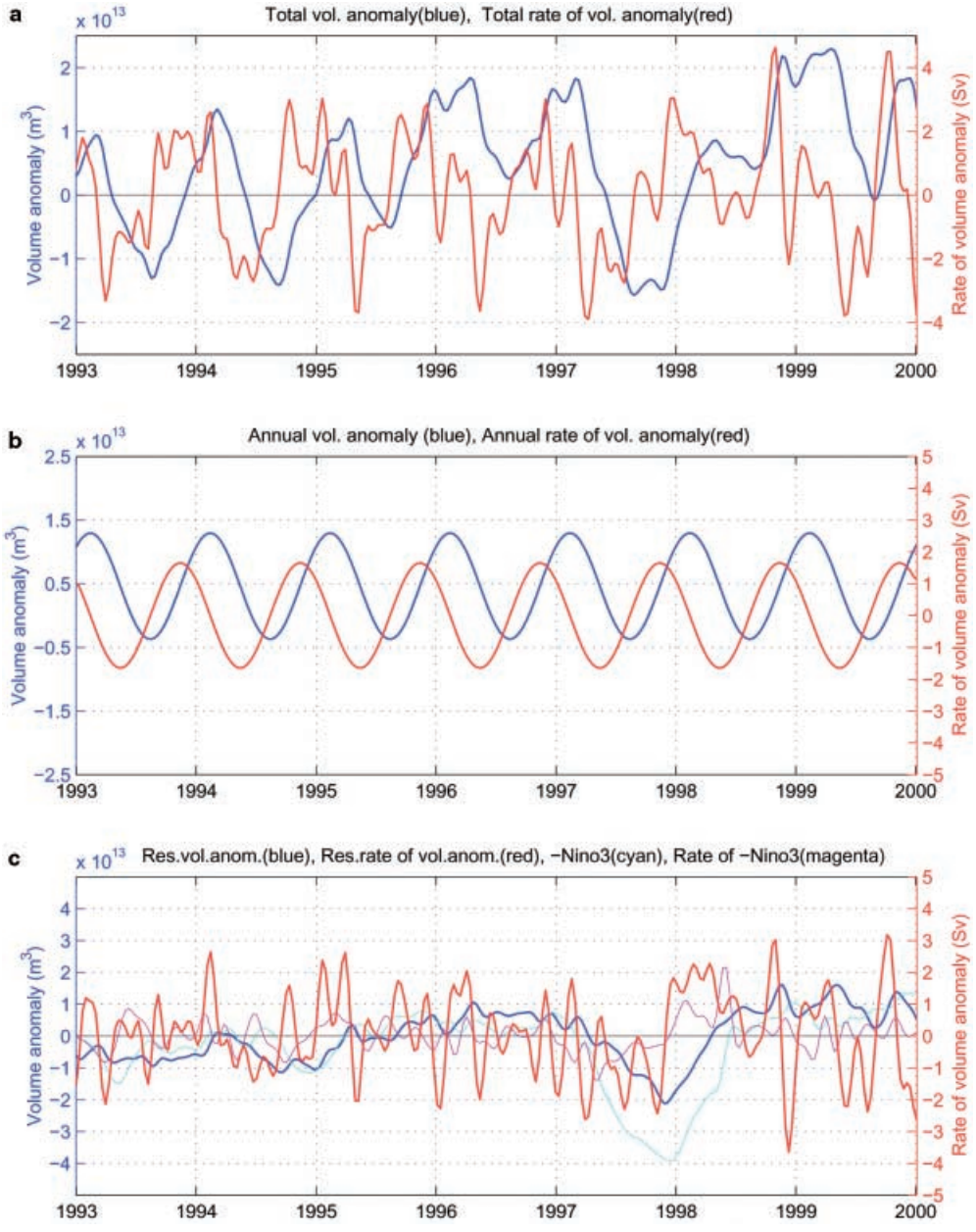

Fig. 5 **a** Time series of the volume anomaly (relative to the 3-year mean) of Banda Sea surface layer (*blue line*, scale in 10^{13} m^3, shown at *left*) and time rate of change of the surface-layer volume anomaly (*red line*, scale in Sverdrups, $Sv = 10^6$ m^3 s^{-1}, shown at *right*) **b** The annual curve of the volume anomaly (*blue line*, scale to *left*) and of the rate of change of the surface anomaly (*red line*, scale in Sv to *right* of figure). **c** The difference between the total and annual curve for the volume anomaly (*blue line*, scale to *left*) and rate of change of the anomaly (*red line*, scale in Sverdrups to the *right*). The (cyan) line is the nino3 index; the (magenta) line is the rate of change of the nino3 index

effects are minor (see above). We assume that the tidal aliasing is also minor, but confirmation must await development of a high-resolution tidal model for the Indonesian seas. The divergence of the surface layer attains values of ± 4 Sv, which is potentially large enough to have an effect on the ITF. The annual average rate of change of the surface-layer volume (Fig. 5b) shows that during the transitional monsoon months maximum values are reached: 1.7 Sv gain (convergence) in October/November, with the matching loss (divergence) in April/May. The divergence of the residual (total–annual; Fig. 5c) weakly correlates with the ENSO (nino3) rate of change. During the El Niño growth period of 1997 the surface layer is strongly divergent, with a net loss of surface water, but in 1998 when the El Niño was on the wane, the average rate of change is convergent.

The total and residual divergence varies significantly at 2- to 3- month, intraseasonal seasonal periods. This is most likely induced by Rossby waves entering the Indonesian seas from the Pacific, and perhaps Kelvin waves from the Indian Ocean (Kashino et al. 1999; Qiu et al. 1999; Sprintall et al. 2000; Susanto et al. 2000). Investigation of intraseasonal phenomena in the Banda Sea is planned.

4 Storage of Indonesian throughflow in the Banda Sea

As the divergence of the surface layer in the Banda Seas can reach 4 Sv, it could influence the phasing of the surface-water transports associated with the ITF. Chong et al. (2000) and Hautala et al. (2001, in press) use a

shallow pressure gauges array (SPGA) across key channels of the Lesser Sunda Islands to estimate the geostrophic export into the Indian Ocean within the upper 100 m for the period from late 1995 to early 1998. According to Wyrtki's (1958) proposal, there should be a correlation between Ekman pumping in the Banda Sea and surface-layer export to the Indian Ocean. Larger surface-water export will occur during the southeast monsoon upwelling (surface-layer divergence) period, with reduced export when the Banda Sea is experiencing Ekman-induced downwelling (convergence), as during the northwest monsoon.

Comparison of the SPGA (Hautala et al. 2001, in press, their Fig. 11) time series does indeed indicate some relationship with Banda Sea surface-layer divergence (Fig. 6). The SPGA record was smoothed to match the altimeter temporal resolution. The SPGA outflow is a combination of the flow through Lombok, Ombai, and Timor passages. During the unfortunate 9-month gap from November 1996 to August 1998 in the Timor Passage data, we used the outflow only from Lombok and Ombai, which degrades the correlation value. The highest correlation of 0.46 (at a significant level of 70%) is found with a 3.3-month lag of the SPGA time series. This lag may be due to the distance between the upwelling center in the eastern Banda Sea and Arafura Sea (Fig. 1c) from the export channels. Using a 600-km mean distance between upwelling center and the export channels, a time lag of 3.3 months requires a mean surface water drift of approximately 0.07 m s^{-1}.

As the Banda Sea surface water may also be exported northward into the Halmahera and Maluku Seas or westward into the Java Sea and Makassar Strait (Wyrtki 1958, 1961), the export to the Indian Ocean does not necessarily close the Banda Sea surface-water mass balance. In addition, the TOPEX/ERS altimeter data may include tidal aliasing, as the tide signals may not have been entirely removed. In consideration of these caveats, as well as the 9-month gap in the Timor Passage record, we consider the correlation of the altimeter and SPGA time series as reasonably good.

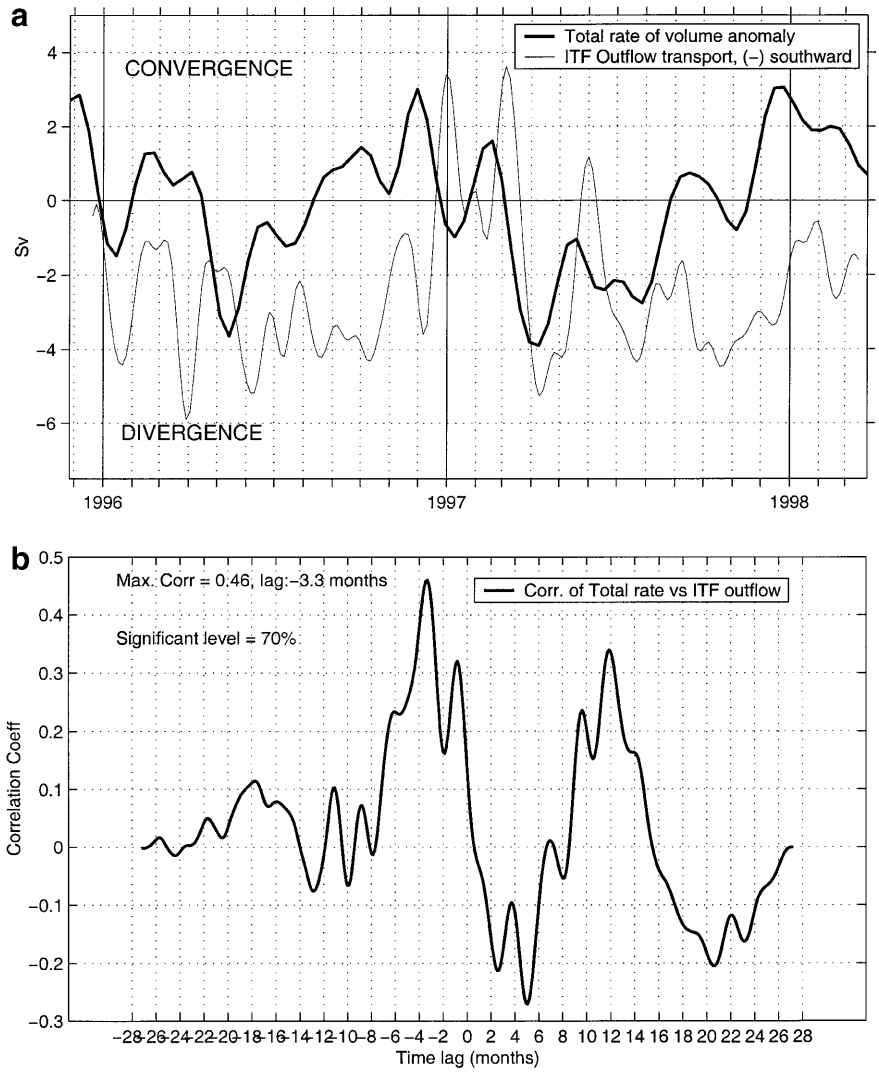

Fig. 6 **a** Banda Sea surface-layer divergence (in Sverdrup, where Sv = 10^6 m^3 s^{-1}; *thicker line*) and the Surface Pressure Gauge Array-estimated transport for the upper 100 m within the major export channels in the Lesser Sunda Archipelago (*thinner line*; Hautala et al. 2001). **b** Lag correlation of Banda divergence to Lesser Sunda export within the upper 100 m

5 Conclusions

The heaving of sea level in the Banda and Arafura Seas, as measured by the T/P-ERS altimeters, is used to estimate the divergence of the surface water within these seas. The altimeter-derived SLA variations represent a combination of mass divergence, steric changes, and tidal aliasing. The regional steric affects are expected to be less than 17% of the signal. Processing of the altimeter data by CLS attempts to remove the tidal signal, but as no high-resolution tidal model exists for the Indonesian seas, some bias due to tidal aliasing may still be present. If the combination of steric and tidal aliasing is a minor contribution to SLA, the divergence of the surface layer within these seas reaches 4 Sv, approximately the transport estimated by the SPGA for the upper 100 m within the channels of the Lesser Sunda Island chain. Therefore the Banda/Arafura divergence has the potential to affect the characteristics of ITF export into the Indian Ocean. The correlation between satellite altimeter-derived Banda/Arafura divergence and the 3.3-month lagged surface-water export to the Indian Ocean, as estimated by the SPGA, is 0.46 at the 70% confidence level. In consideration of the various uncertainties, including the 9-month gap in the SPGA Timor Passage record, the correlation provides reasonable encouragement that satellite altimetry can indeed be used to study aspects of the ITF.

Our calculations suggest that Banda surface-layer divergence does indeed influence the timing and transport profile of the ITF export into the Indian Ocean, as proposed by Wyrtki (1958). Waworuntu et al. (2000) suggest that the stratification and water mass composition in the Banda Sea and surrounding seas is affected by the Banda divergence. Hautala et al. (2001, in press) suggest that divergence within the Banda Sea thermocline would have important effects on thermocline stratification and upper ocean heat content. The Banda Sea acts as a ''capacitor'' in controlling the timing of surface-layer export to the Indian Ocean, and must be taken into account in ITF research.

Continued evaluation of the use of satellite altimeter data for the study of the ITF is advocated. This includes comparison of these products with in situ-derived data, such as obtained by the SPGA, repeat XBT sections, and time series from moorings, and the development of a high-resolution tidal model for the Indonesian seas to remove tidal aliasing.

Acknowledgement We appreciate the support of NASA grant NAG 5-8297 and JPLCIT 1228179, and thank CLS Space Oceanography Division, CNES, for providing the T/P ERS sea-level data. We are grateful to Susan Hautala for providing a preprint of Hautala et al. (2001), which includes the Shallow Pressure Gauge Array time series used in Fig. 6. Lamont–Doherty Earth Observatory contribution number 6228.

References

Bray NA, Hautala S, Chong J, Pariwono J (1996) Large-scale sea level, thermocline, and wind variations in the Indonesian throughflow region. J Geophys Res 101: 12239–12254

Chong J, Sprintall J, Hautala S, Morawitz W, Bray N, Pandoe W (2000) Shallow throughflow variability in the outflow straits of Indonesia. Geophys Res Lett 27: 125–128

Ffield A, Gordon AL (1996) Tidal mixing signatures in the Indonesian seas. J Phys Oceanogr 26: 1924–1937

Ffield A, Vranes K, Gordon AL, Susanto RD, Garzoli SL (2000) Temperature variability within Makassar Strait. Geophys Res Lett 27: 237–240

Gordon AL (2001) Interocean exchange. In: Siedler G, Church J, Gould J (eds) Ocean circulation and climate, Chap 4.7, Academic Press, New York, pp 303–314

Gordon AL, Fine RA (1996) Pathways of water between the Pacific and Indian oceans in the Indonesian seas. Nature 379: 146–149

Gordon AL, Susanto RD, Ffield AL (1999) Throughflow within Makassar Strait. Geophys Res Lett 26: 3325–3328

Hautala S, Sprintall J, Potemra J, Ilahude A, Chong J, Pandoe W, Bray N (2001) Velocity structure and transport of the Indonesian throughflow in the major straits restricting flow into the Indian Ocean. J Geophys Res (in press)

Ilahude AG, Gordon AL (1996) Thermocline stratification within the Indonesian seas. J Geophys Res 101: 12401–12409

Kalnay E, et al (1996) The NCEP/NCAR 40-year reanalysis project. Bull Am Meteorol Soc March

Kashino Y, Watanabe H, Herunadi B, Aoyama M, Hartoyo D (1999) Current variability at the Pacific entrance of the Indonesian throughflow. J Geophys Res 104: 11021–11035

Le Provost C (2001) Ocean tides In: Fu LL, Cazenave A (eds) Satellite altimetry and earth sciences, a handbook of techniques and applications, Academic Press, New York, 463 pp

Le Traon PY, Nadal F, Ducet N (1998) An improved mapping method of multi-satellite altimeter data. J Atm Ocean Techn 25: 522–534

Qiu B, Mao M, Kashino Y (1999) Intraseasonal variability in the Indo-Pacific throughflow and the region surrounding the Indonesian seas. J Phys Oceanogr 29: 1599–1618

Reynolds RW, Smith TM (1994) Improved global sea surface temperature analyses. J Climate 7: 929–948

Sprintall J, Gordon A, Murtugudde R, Susanto RD (2000) A semi-annual equatorial western Indian Ocean forced Kelvin wave observed in the Indonesian seas in May 1997. J Geophys Res 105: 17217–17230

Susanto RD, Gordon A, Sprintall J, Herunadi B (2000) Intraseasonal variability and tides in Makassar Strait. Geophys Res Lett 27: 1499–1502

Tomczak M, Godfrey JS (1994) Regional oceanography: an introduction Pergamon Press, London, 422 pp

Waworuntu J, Fine R, Olson D, Gordon A (2000) Recipe for Banda Sea water. J Mar Res 58: 547–569

Wyrtki K (1958) The water exchange between the Pacific and the Indian Oceans in relation to upwelling process. Proceedings of the Ninth Pacific Science Congress, Inst Mar Res, Djakarta, Indonesia, 16: 61–65

Wyrtki K (1961) Physical oceanography of Southeast Asian waters. NAGA Rep. 2, 195 pp